

# Data acquisition from digital holograms of particles

Victor V. Dyomin\*<sup>a</sup>, Alexey S. Olshukov<sup>a</sup>, Alexandra Y. Davydova<sup>a</sup>

<sup>a</sup>National Research Tomsk State University, 36, Lenin Ave., Tomsk 634050, Russian Federation

## ABSTRACT

A technique for data acquisition from digital holograms of particle ensembles, including preprocessing of the digital hologram, construction of a two-dimensional display of the holographic image of investigated volume, and segmentation and measurement of particle characteristics is considered. The proposed technique is realized in automatic regime and can work in real time. Results of the technique approbation using digital holograms of sand, plankton particles in water, and air bubbles in oil are presented.

**Keywords:** digital holography, data acquisition, plankton investigation, submersible holocamera, image processing, particles recognition

## 1. INTRODUCTION

Digital holography is widely used to study particles [1–8], including planktonic species in their habitat, with underwater holocameras. The main task in the study of particle ensembles is the determination of integral characteristics [9–10] such as the concentration, particle distribution in space, and particle size distribution. However, in some cases, for example, in the study of plankton, in addition to the integral characteristics, information on individual planktonic species is required, including particle size, shape, orientation, spatial position, velocity, and trajectory of motion [10–16]. In addition, to assess the ecological state of water area, it is necessary to solve the problem of plankton identification, because information on the plankton species ratio in this case is important [11–18]. The use of digital holography and special software for processing of digital holograms is highly efficient for solving similar problems [1–7, 9–11, 18–19]. A digital hologram contains sufficient and in some cases even excessive information about each particle in the investigated volume. In this paper we consider a technique for obtaining information about investigated particles from digital holograms and its representation.

To retrieve information about the investigated particles from the digital hologram, the following steps are necessary:

- 1) Preprocessing of the digital hologram (by removal or leveling of the background and suppression of the edge noise using cubic spline approximation),
- 2) Reconstruction of a preset number of images of the cross-sections of investigated volume with particles from the digital hologram and construction of their two-dimensional (2D) displays,
- 3) Improvement of the quality and binarization of 2D displays,
- 4) Automatic selection of particle image and determination of the characteristics of each particle and integral characteristics of a particle ensemble.

For further interpretation of the results, a technique for automatic recognition of basic taxonomic groups of plankton particles is required.

Let us consider each step in more detail using digital particle holograms. The parameters of recording of digital holograms were the same for all types of particles: in-line registration scheme (Figure 1), wavelength of 0.66  $\mu\text{m}$ , matrix pixel size of 5.5  $\mu\text{m}$ , pixel size in reconstructed image of 15.5  $\mu\text{m}$  (determined by the procedure of calibration using standard model objects with known sizes), size of the camera matrix of 2048  $\times$  2048 pixels, but for clarity, this article presents framed images of 1024  $\times$  1024 pixels.

\*dyomin@mail.tsu.ru; phone +3822529601; fax +3822529585

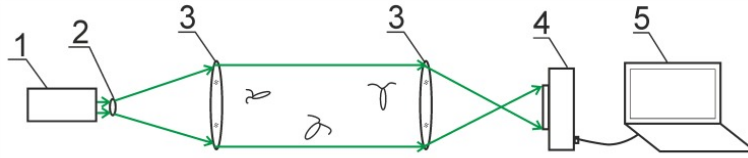


Figure 1. In-line scheme for recording digital holograms comprising laser 1, lenses 2 and 3, CCD/CMOS camera 4, and computer 5.

## 2. DIGITAL HOLOGRAM PREPROCESSING

The first stage of digital hologram preprocessing consists of removing irregular background illumination or static background caused by diffraction on contaminations or inhomogeneities of the optical components that may arise during holographing under field conditions. One of the two methods can be used to suppress the irregular and static backgrounds: 1) recording a digital hologram without object under study (*empty* hologram without particles) and subtracting it from the digital hologram with particles, and 2) subtraction of the digital hologram averaged over several holograms recorded subsequently from the digital hologram. If there is a technical possibility of recording of the hologram without objects (particles), then the first method is used. Thus, the digital hologram without sand was subtracted from the hologram of a sand monolayer (Figure 2 (a)), and the result is shown in Figure 2 (d). Another example is the digital hologram of plankton particles in the cell with water (Figure 2 (b)). The digital hologram of the cell with water and without plankton particles (when plankton species escaped from the frame) was used as an empty hologram (result of background subtraction is shown in Figure 2 (e)). The second method is used when it is impossible to register an empty hologram and only for moving particles. An example of application of the second method is shown in Figures 2 (c) and (f) – the digital hologram of air bubbles gradually rising upwards in oil. Five holograms were averaged and subtracted from the digital hologram in Figure 2 (c), and the result is shown in Figure 2 (f).

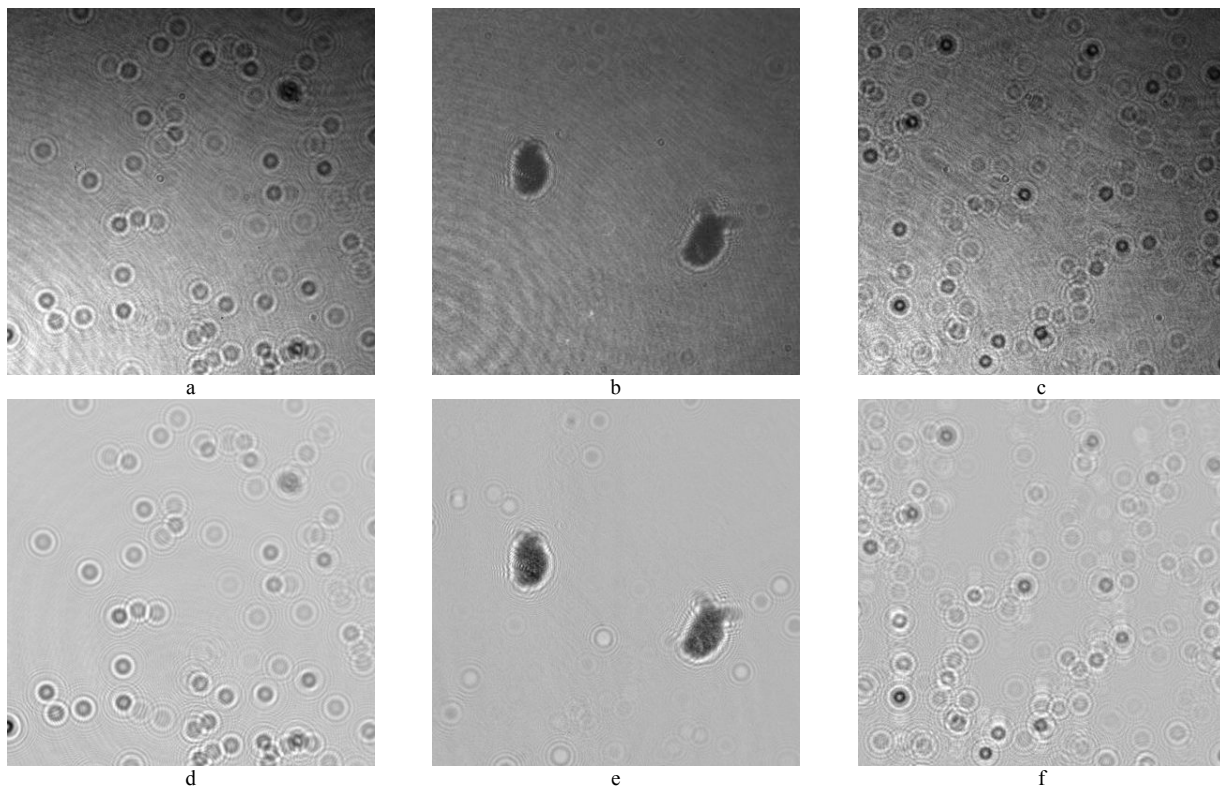


Figure 2. Digital holograms before and after suppression of the irregular and static backgrounds: holograms of a sand monolayer before (a) and after (b) background subtraction; holograms of plankton species before (b) and after (e) subtraction of the empty hologram; and holograms of air bubbles in oil before (c) and after (f) subtraction of the hologram averaged over a series of five holograms.

The results of image reconstruction from digital holograms without preliminary processing of the hologram background are shown in Figures 3 (a) and (c). The effect of irregular background illumination and diffraction on contamination of optical components of the registration scheme is clearly pronounced in Figure 3 (c) which illustrates the image reconstructed from a digital hologram recorded during the Mission in the Kara Sea. The presence of noise complicates the subsequent particle selection and determination of the particle characteristics. In this example, to remove the background from the digital hologram, the second method was used, namely, the subtraction of the average digital hologram. As a result of background removal from the digital hologram, the quality of the restored image significantly improved (Figure 3 (d)). Figure 3 (b) shows image 3 (a) improved by subtraction of the empty hologram from the initial hologram using the first method described above. All the images shown in Figure 3 are two-dimensional displays of holographic images of investigated volume, and the algorithm of their construction is described in Section 3.

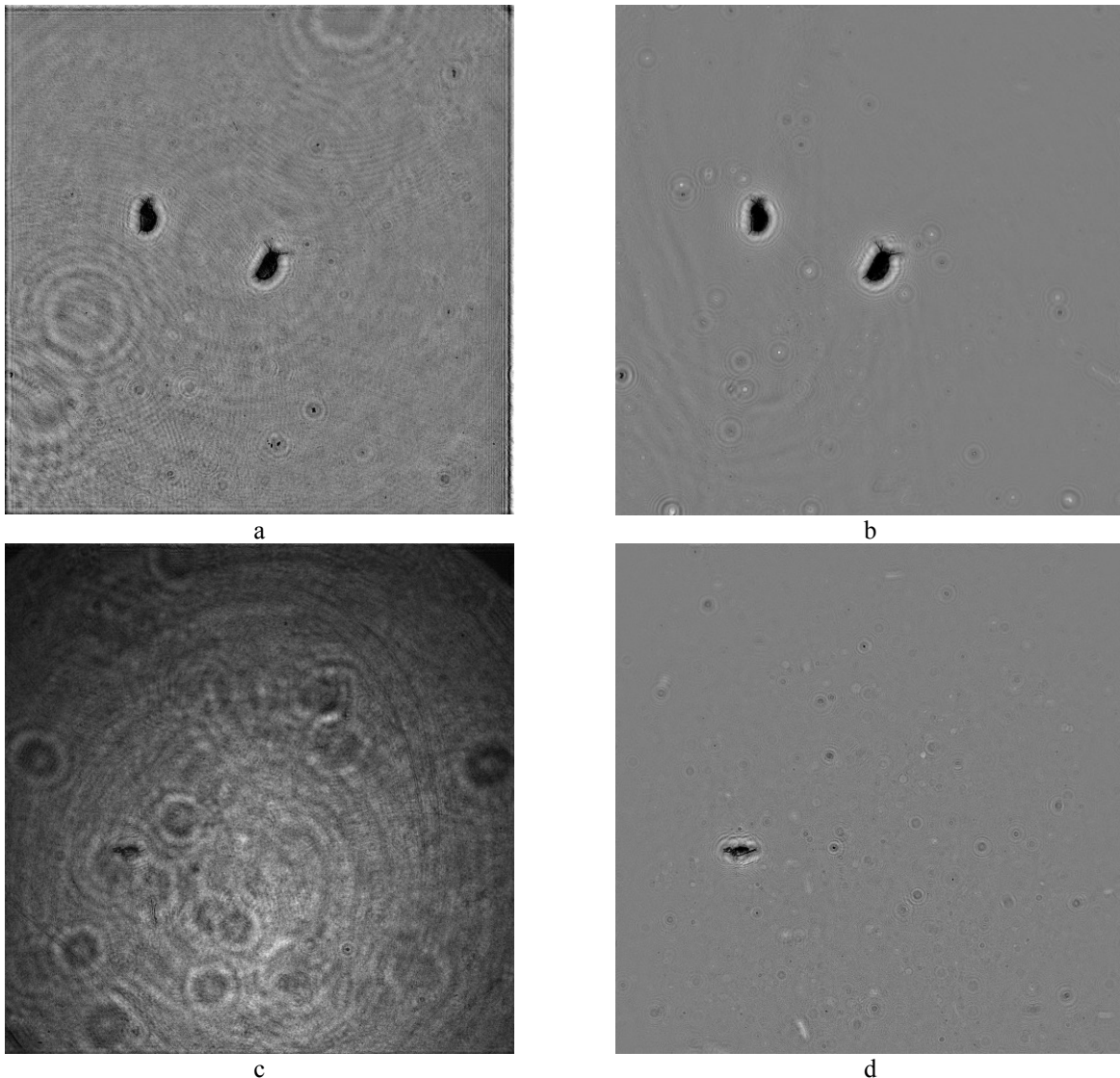


Figure 3. Two-dimensional display of the holographic image of investigated volume with plankton particles, reconstructed from a digital hologram that was not subjected to background preprocessing and recorded under laboratory conditions (a) and during the Mission in the Kara Sea (c). Reconstructed images (b) and (d) after holograms preprocessing.

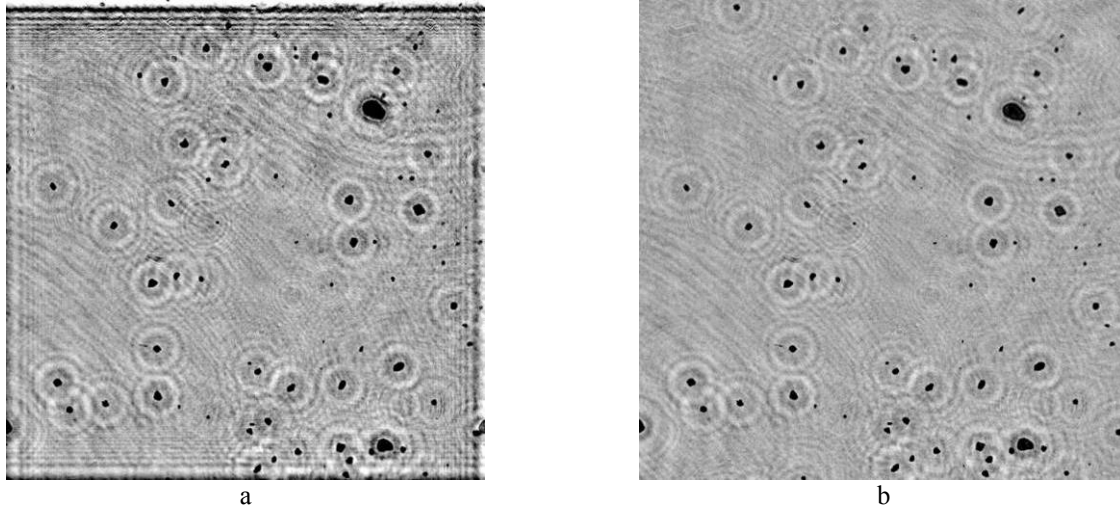


Figure 4. (a) Reconstructed image of a monolayer of sand particles without preliminary extrapolation of the digital hologram. Diffraction bands duplicating the contour of the frame and distorting images of sand particles are present on the image. (b) Reconstructed image of the monolayer of sand particles after preliminary extrapolation of the digital hologram by bicubic splines.

It is well known that a digital hologram is registered on a CCD (or CMOS) matrix and represents a discrete and bounded two-dimensional array of the intensities (see Figure 2). The discrete and bounded data character lead to the appearance of noise (or distortion) of images reconstructed from the digital hologram. One type of such noise is the system of diffraction bands duplicating the contour of the frame (Figure 4 (a); this is the image of the monolayer of sand particles reconstructed from the hologram without preliminary extrapolation). The superimposition of bands on the particle image may hinder the selection of particle image and the determination of particle parameters. To suppress the examined edge noise, it is necessary to increase the size of the digital hologram by filling new pixels with gray values using bicubic spline extrapolation [20]. The reconstructed image of sand particles after extrapolation of the digital hologram is shown in Figure 4 (b).

### 3. 2D DISPLAY OF THE HOLOGRAPHIC IMAGE OF INVESTIGATED VOLUME

The next step after the digital hologram preprocessing is the reconstruction of images from the digital hologram and obtaining information about particles. The process of layer-by-layer numerical reconstruction of the image of investigated volume from the digital hologram is well known. However, there is usually no need to store information about the entire volume in the form of a set of images reconstructed in different layers; it takes a lot of disk space on the computer. It is sufficient to form one image in which all particle images will be in focus. In this paper, we pay attention to the construction of this two-dimensional display of the holographic image of investigated volume.

To automatically construct the two-dimensional display of the holographic image of investigated volume, we propose to decompose each image of the volume cross-sections reconstructed for different layers into segments of a fixed size using one and the same grid. Thus, longitudinal blocks are formed from segments with identical transverse coordinates. For each block, the plane of the best focusing of particle image or its fragment is determined using the Tenengrad method [21–22]. Using the focused images located in these segments (with the maximum value of the Tenengrad operator), a resulting two-dimensional display of the holographic image of investigated volume is compiled.

The brightness of the reconstructed holographic images may differ in different layers, so that the intensity difference may arise in the compiled two-dimensional display at the segment boundaries (Figure 5). Therefore, additional processing of the reconstructed images of layers is required, which consists in equalizing image illumination using the Retinex algorithm [23]. This algorithm allows equalizing illumination of all restored images. Filtering is carried out according to the following formula:

$$R(x, y, \sigma) = \log(I(x, y)) - \log(I(x, y) * G(x, y, \sigma)),$$

where  $G$  is the Gaussian filter [24],  $\sigma$  is the blur coefficient,  $*$  is the convolution operator,  $(x, y)$  are coordinates of the current pixel.

After filtration, most of the resulting pixels have the intensity values in the range  $[-1; 1]$ ; to visualize the image, these values should be normalized according to the formula:

$$I_R(x, y) = 255 \times R(x, y, \sigma) + 127.$$

In addition, due to the nonlinear normalization of the image, the contrast of the image increases, thereby improving the process of extracting information about the investigated particles in the next stage. In this paper, reconstructed images after the Retinex filtering were used to construct a two-dimensional display of the holographic image of investigated volume.

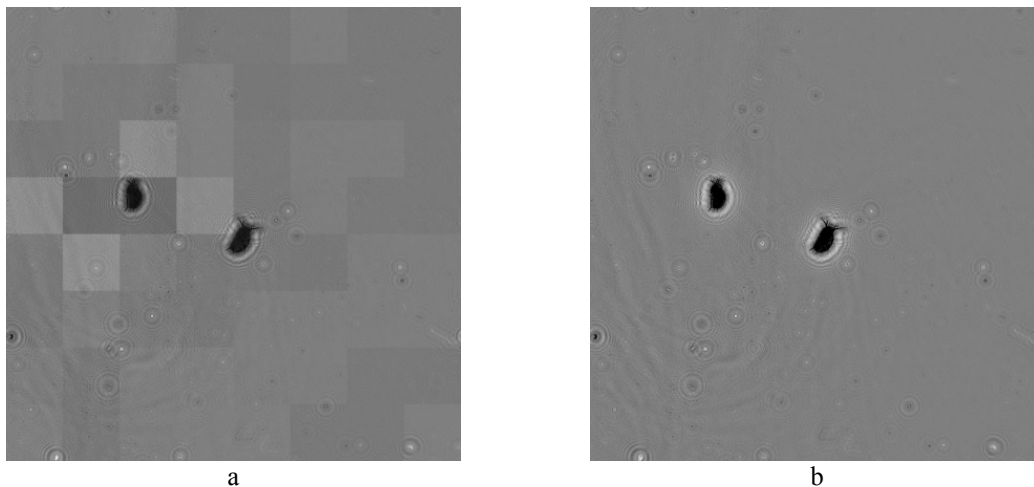
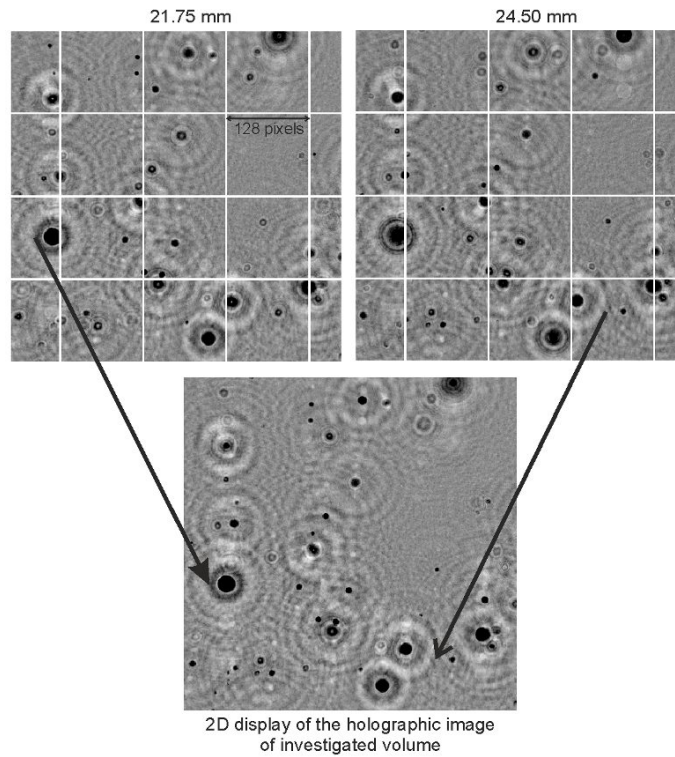


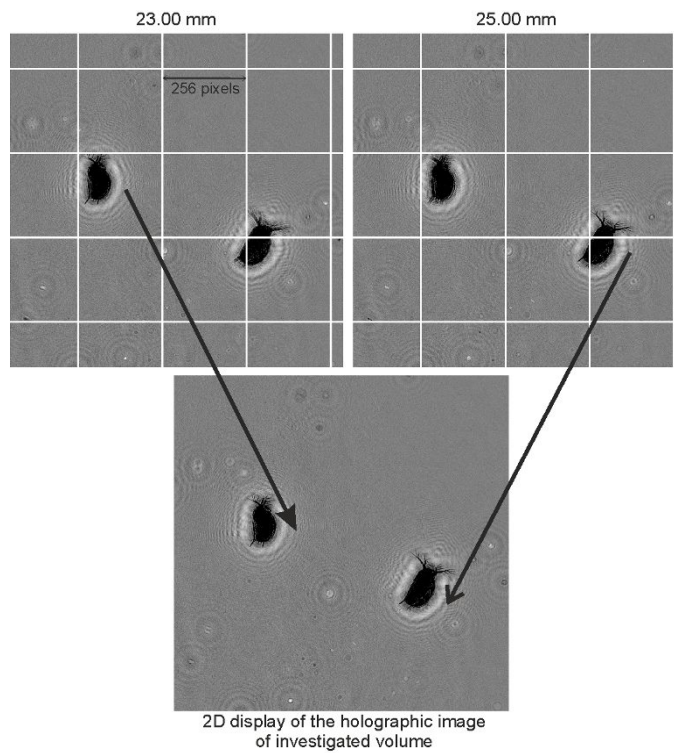
Figure 5. Two-dimensional display of the holographic image of investigated volume formed (a) without additional processing of the reconstructed images and (b) using the reconstructed images of the layers after the Retinex filtration.

The reconstructed images with a schematic designation of the segment edges and the constructed two-dimensional display are shown in Figure 6. The segments selected to form a two-dimensional display are indicated in the figures. The images of investigated volume cross-sections were reconstructed from the digital hologram at distances from 14 to 29 mm with increment of 0.25 mm, i.e., one longitudinal block consists of 60 layers. The images with air bubbles in oil in Figure 6 (a) are framed and enlarged for clarity, and the image size in Figure 6 (a) is  $512 \times 512$  pixels. The size of the image in Figure 6 (b) is the same as in previous figures –  $1024 \times 1024$  pixels.

The choice of the segment size depends on the size of investigated particles: the size of the transverse grid segment must be commensurate with that of the particle under study. Thus, for air bubbles in oil the segment size was  $128 \times 128$  pixels, and for plankton particles it was  $256 \times 256$  pixels.



a



b

Figure 6. Constructing the two-dimensional display of the holographic image of investigated volume (a) with air bubbles in oil and (b) with planktonic particles in water.

The next step is to obtain information about particles under study. The time of processing of the resulting two-dimensional display of the holographic image of investigated volume with particles is less than the time of processing of each of the restored images in different volume cross-sections (in our examples, 60 images).

First of all, it is necessary to select particle images in the 2D display. For this purpose, automatic (without participation of the operator) threshold determination is used for binarization of the 2D image. The global binarization threshold is determined based on an analysis of the image histogram: a critical point is searched where the derivative of the function describing the plot of the histogram is equal to 0. Because the histogram of the image is a discrete function of discrete argument, the search algorithm determines the point where the derivative is less than 5% (this level was determined empirically) of the derivative value at the maximum of the histogram rather than zero. Figure 7 shows the histogram of the two-dimensional display shown in Figure 6 (b). In this case, the global software-defined binarization threshold was 77.

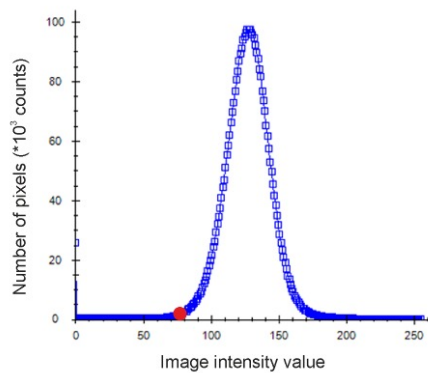


Figure 7. Histogram for the image shown in Figure 6 (b). The red circle indicates the software-defined binarization threshold (equal to 77).

Using the automatically selected threshold, the binarization is performed. The noise in the binarized images of the “salt and pepper” type has a 1 pixel size. This noise is removed by subsequent application of the morphological dilatation and erosion operations. Then each particle is selected in the binarized image. The selection method determines pixels belonging to the image of the given particle, and after its application, the current particle is colored differently compared to the color of the background and other particles (in this option, the particle is colored gray with the image intensity value equal to 150, whereas the background image intensity value is equal to 255 and values of the image intensities of other particles are equal to zero). The results of threshold binarization, dilatation, and erosion and an example of particle selection are shown in Figure 8. The selected particle is circumscribed by the rectangle whose parameters determine the particle parameters (the red rectangle in Fig. 8).

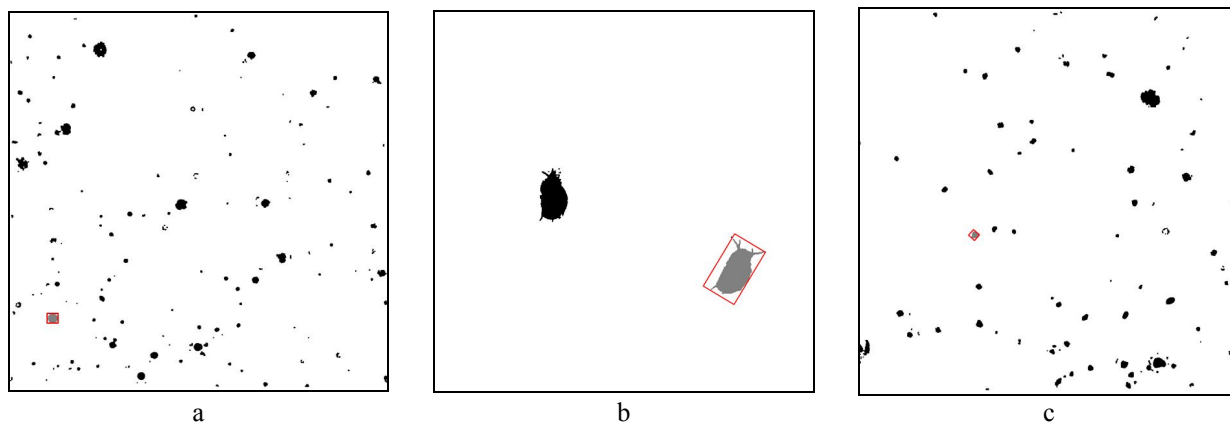


Figure 8. Result of binarization and dilatation and erosion operations (a); particle selection (b, gray color). The rectangle circumscribing the selected particle is marked in red.

In the selected particle image, its length, width, tilt angle, coordinates of the image center of gravity, and area of the image and length of the image boundary are determined.

When constructing a two-dimensional display of the holographic image of investigated volume with particles, the longitudinal coordinates of the planes of best focusing are stored for each segment. Therefore, the information is available about all three coordinates of the center of gravity of each particle image.

The compactness (the ratio of the squared length of the boundary to the square of the particle image), the morphological parameter (the ratio of the width to the length of the particle), and the presence of antennas or other limbs are simultaneously determined for each particle. To determine the presence of the antenna, it is necessary to compare the length of the particle with its length after application of dilatation and erosion operations, when the antennas disappeared. The number of dilatation and erosion operations for antenna removal is determined automatically based on the particle size.

Once all the particle parameters have been determined, the particle image is removed from the binarized image (by the same selection method, but the particle is colored white), and the algorithm considers the next particle and works until all particles escape from the binarized image. The information about the particles obtained in this way forms a database.

As a result of all operations, we obtain information about each particle in the volume. From these data, the integral characteristics of the volume with particles can be analyzed, for example, the particle size distribution (Figure 9).

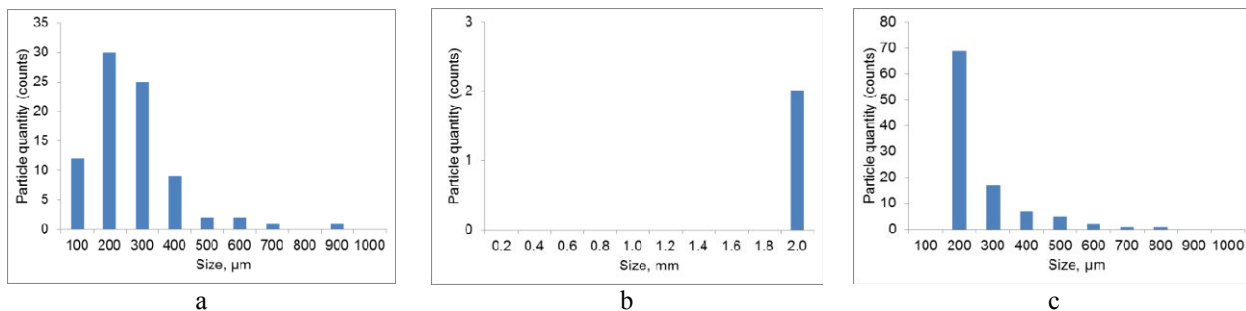


Figure 9. Size distribution: (a) sand monolayer particles, (b) planktonic species Daphnia, (c) air bubbles in the oil.

In addition, the 2D representation of the holographic image of volume with particles instead of separate reconstructed particle images allows the process of video creation based on the holographic data retrieved from the video sequence of holograms to be automated [25].

#### 4. AUTOMATIC CLASSIFICATION OF MARINE PARTICLES

Additional particle parameters, such as the morphological parameter and the presence of antennas, are important for the automatic classification of planktonic particles by basic taxonomic features. Approbation of the implemented method of automatic classification on the results obtained during the Mission in the Kara Sea showed the necessity of using the second parameter – the presence of antennas – in addition to the morphological parameter of the particle. The introduction of the second parameter increased the correctness of classification to 73% [19, 26]. The decision tree of the classifier used for processing of data obtained during the Mission in the Kara Sea is shown in Figure 10.



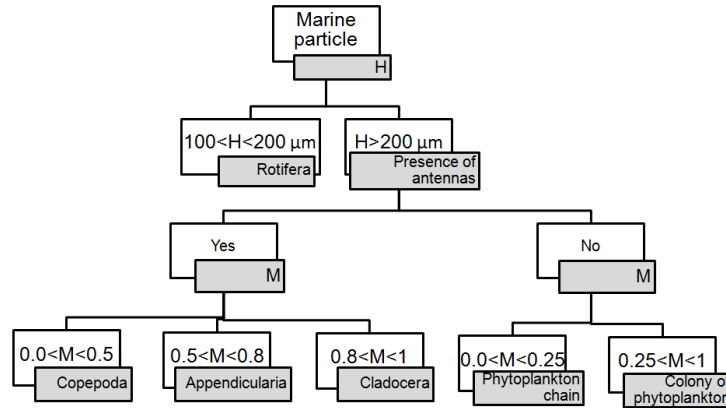


Figure 10. Decision tree of the classifier. Here H is the length and M is the width of the circumscribed rectangular.

The result of classification for plankton species *Daphnia* is shown in Figure 11. The software for automatic classification of plankton places a rectangle with the color of the corresponding taxon (in Figure 11 it is the red color corresponding to the Cladocera taxon) around the particle, and also stores information about the taxon of the particle in the database.

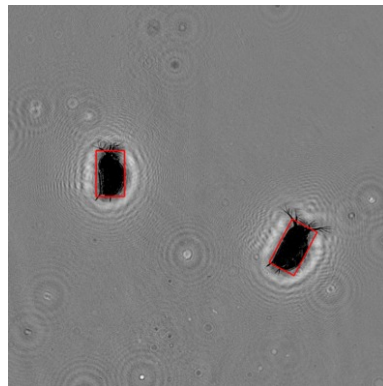


Figure 11. Result of the automatic plankton classification. The red rectangle marks the taxon Cladocera.

## 5. CONCLUSIONS

The above-described technique for processing and acquisition of data from digital holograms is fully automatic. The operator's participation is required only to specify the registration parameters (wavelength, pixel dimensions of the camera and reconstructed image, and reconstruction range and step size) and the transverse segment size (grid cell size) for constructing a two-dimensional display of the holographic image of investigated volume. The classification of particles requires preliminary training (definition of the morphological parameters) of the classifier. Modern computing facilities and special libraries for image processing allow the above-described processing of data to be performed in real time. The joint application of the methods of digital holography and numerical data processing is a promising tool for contactless research of the integral characteristics of ensembles of various particles and also for the determination of the characteristics of individual particles, including their classification.

## ACKNOWLEDGMENTS

The work was carried out within the framework of the Federal Program "Research and Development in Priority Areas of Advancement of the Russian Scientific and Technological Complex for 2014–2020" No. 14.578.21.0205 of 03.10.2016 (unique identifier of the Agreement RFMEFI157816X0205).

## REFERENCES

- [1] Watson, J., "Submersible digital holographic cameras and their application to marine science," *Optical Engineering* 50(9), 091313 (2011).
- [2] Rotermond, L. M., Samson, J., Kreuzer, H. J., "A Submersible Holographic Microscope for 4-D In-Situ Studies of Micro-Organisms in the Ocean with Intensity and Quantitative Phase Imaging," *J Marine Sci Res Dev* 6(1), 181 (2016).
- [3] Bochdansky, A.B., Jericho, M.H., Herndl, G.J., "Development and deployment of a point-source digital inline holographic microscope for the study of plankton and particles to a depth of 6000 m," in *Limnol. Oceanogr.: Methods* 11, 28–40 (2013).
- [4] Talapatra, S., Hong, J., McFarland, M., Nayak, A. R., Zhang, C., Katz, J., Sullivan, J., Twardowski, M. S., Rines, J., Donaghay, P., "Characterization of biophysical interactions in the water column using in situ digital holography," *Marine Ecol. Prog. Ser.* 473, 29-51 (2013).
- [5] Liu, Z., Watson, J., Allen, A., "Efficient image preprocessing of digital holograms of marine plankton," *IEEE Journal of Oceanic Engineering* 43(1), 83-92 (2017)
- [6] Dyomin, V. V., Polovtsev, I. G., Kamenev, D. V., Kozlova, A. S., Olenin, A. L., "Plankton investigation in the Kara Sea by a submersible digital holocamera," *OCEANS 2017 - Aberdeen, Aberdeen*, 1-4 (2017).
- [7] Tan, S., Wang, S., "An approach for sensing marine plankton using digital holographic imaging," *Optik - International Journal for Light and Electron Optics* 124, 6611-6614 (2013).
- [8] Wiebe, P.H., Benfield, M.C., "From the Hensen net toward four-dimensional biological oceanography," *Prog. Oceanogr.* 56(1), 7-136 (2003).
- [9] Vovk, T. A., Petrov, N. V., "Correlation Characterization of Particles in Volume Based on Peak-to-Basement Ratio," *Sci. Rep.* 7, 43840 (2017).
- [10] Dyomin, V. V., Kamenev, D. V., "Investigation of particles located in the water by digital holography," *Proc. SPIE 9771, Practical Holography XXX: Materials and Applications, 97710H* (7 March 2016).
- [11] Katz, J., Sheng, J. "Application of Holography in Fluid Mechanics and Particle Dynamics," *Annu. Rev. Fluid Mechanics* 42, 531-555 (2010).
- [12] Cowen, R. K., Guigand, C. M., "In situ ichthyoplankton imaging system (ISIIS): system design and preliminary results," *Limnol. Oceanogr.: Methods* 6, 126–132 (2008).
- [13] Gorsky, G., Ohman, M. D., Picheral, M., Gasparini, S., Stemmann, L., Romagnan, J. B., Cawood, A., Pesant, S., García-Comas, C., Prejger, F., "Digital zooplankton image analysis using the ZooScan integrated system," *J. Plankton Res.* 32(3), 285–303 (2010).
- [14] Grosjean, P., Picheral, M., Warembourg, C., Gorsky, G., "Enumeration, measurement, and identification of net zooplankton samples using the ZOOSCAN digital imaging system," *ICES J. Mar. Sci.* 61, 518–525 (2004).
- [15] Le Bourg, B., Cornet-Barthaux, V., Pagano, M., Blanchot, J., "FlowCAM as a tool for studying small (80-1000  $\mu$  m) metazooplankton communities," *Journal of Plankton Research* 37(4), 666-670 (2015).
- [16] Vandromme, P., Stemmann, L., Garcia-Comas, C., Berline, L., Sun, X., Gorsky, G., "Assessing biases in computing size spectra of automatically classified zooplankton from imaging systems: A case study with the ZooScan integrated system," *Methods in Oceanography* 1-2, 3-21 (2012).
- [17] Sieracki, M. E., Benfield, M., Hanson, A., Davis, C., Pilskaln, C. H., Checkley, D., Sosik, H. M., Ashjian, C., Culverhouse, P., Cowen, R., Lopes, R. M., Balch, W., Irigoien, X., "Optical plankton imaging and analysis systems for ocean observation," *OceanObs 09, 2010, Venice. Proceedings of OceanObs 09: Sustained Ocean Observations and Information for Society*, ESA Publication WPP-306. Paris : European Space Agency, 2 (2010).
- [18] Zetsche, E.-M., El Mallahi, A., Dubois, F., Yourassowsky, C., Kromkamp, J. C., Meysman, F. J.R., "Imaging-in-Flow: Digital holographic microscopy as a novel tool to detect and classify nanoplanktonic organisms," *Limnol. Oceanogr.: Methods* 12, 757–775 (2014).
- [19] Dyomin, V. V., Polovtsev, I. G., Davydova, A. Yu., "Physical principles of the method for determination of geometrical characteristics and particle recognition in digital holography," *Russian Physics Journal* 60(11) 2044-2046 (2018).
- [20] Dyomin, V. V., Olshukov, A. S., "Improvement of the Quality of Reconstructed Holographic Images by Extrapolation of Digital Holograms," *Russian Physics Journal* 58(10), 1413-1419 (2016).

- [21] Dyomin, V. V., Kamenev, D. V., "Two-dimensional representation of a digital holographic image of the volume of a medium with particles as a method of depicting and processing information concerning the particles," *J. Opt. Technol.* 80(7), 450-456 (2013).
- [22] Dyomin, V. V., Kamenev, D.V., "Evaluation of Algorithms for Automatic Data Extraction from Digital Holographic Images of Particles," *Russian Physics Journal* 58(10), 1467-1474 (2016).
- [23] Petro, A. B., Sbert, C., Morel, J.-M., "Multiscale Retinex," *Image Processing On Line*, 71–88 (2014).
- [24] Pratt, W. K. [Digital image processing : PIKS Scientific inside] Wiley-Interscience, 4th ed.(2007).
- [25] Dyomin, V.V., Olshukov A.S., "Digital holographic video for studying biological particles," *J. Opt. Technol.* 79, 344-347 (2012)
- [26] Dyomin, V.V., Polovtsev, I.G., Davydova, A.Y., "Fast recognition of marine particles in underwater digital holography," *Proc. of SPIE* 10466, 1046627-1-1046627-5 (2017).